



## Highly polarised electroluminescence in low aspect ratio mesogenic molecules

Sa-Wook Kim, Dong-Myoung Lee, Jae-Hoon Kim, E-Joon Choi & Chang-Jae Yu

To cite this article: Sa-Wook Kim, Dong-Myoung Lee, Jae-Hoon Kim, E-Joon Choi & Chang-Jae Yu (2019): Highly polarised electroluminescence in low aspect ratio mesogenic molecules, Liquid Crystals, DOI: [10.1080/02678292.2018.1558465](https://doi.org/10.1080/02678292.2018.1558465)

To link to this article: <https://doi.org/10.1080/02678292.2018.1558465>



Published online: 07 Jan 2019.



Submit your article to this journal [↗](#)



Article views: 67



View Crossmark data [↗](#)



# Highly polarised electroluminescence in low aspect ratio mesogenic molecules

Sa-Wook Kim<sup>a\*</sup>, Dong-Myoung Lee<sup>b\*</sup>, Jae-Hoon Kim<sup>b</sup>, E-Joon Choi<sup>a</sup> and Chang-Jae Yu<sup>b</sup>

<sup>a</sup>Department of Polymer Science and Engineering, Kumoh National Institute of Technology, Gumi, South Korea; <sup>b</sup>Department of Electronic Engineering, Hanyang University, Seoul, South Korea

## ABSTRACT

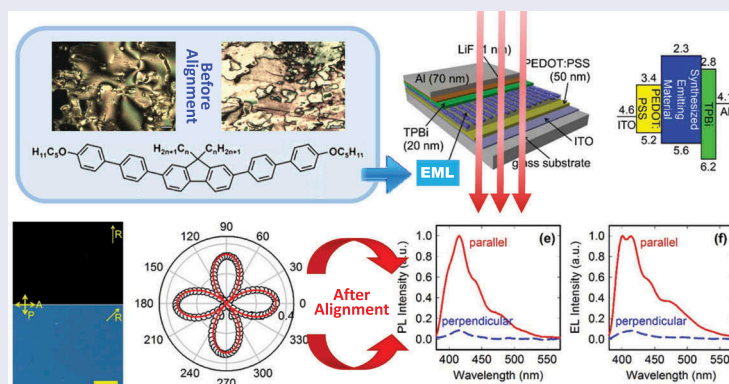
We have synthesised the low aspect ratio mesogenic compounds containing one fluorene and two biphenyl moieties, and investigate their mesomorphic properties and the resultant anisotropic properties in both photoluminescence and electroluminescence. We introduced pentyloxy as a terminal flexible group in order to guarantee formation of mesophase and varied the lateral flexible group from propyl to octyl to control the mesogenic transition temperature. Eventually, in spite of the low aspect ratio mesogen, high polarisation ratio (PR) was achieved by spin-coating of luminescent nematogenic molecules. Furthermore, the PR was significantly enhanced by the additional thermal annealing process.

## ARTICLE HISTORY

Received 16 November 2018  
Accepted 8 December 2018

## KEYWORDS

Electroluminescence;  
photoluminescence; liquid  
crystal; polarised emission



## 1. Introduction

Liquid crystalline (LC) property in the organic light-emitting diodes (OLEDs) has attracted much attention in the research field of next generation displays since polarised electroluminescence (EL) based on ordered materials gives rise to an enhancement of display efficiency [1–15]. Over the past few decades, a considerable number of studies have been made on the high quantum efficiency of EL property for poly(fluorene)s as well as oligo(fluorene)s [6–9,16–18]. From a structural point of view, the fluorene ring system has been considered as one of the prospective candidates for practical luminescent mesogen since it possesses high luminescence yield, good solubility in solvents, and potentially LC characteristics. There are many reports on the relationship between molecular structure and mesogenic property for the poly(fluorene)s including oligo(fluorene)s analogues can be found in the literatures [16–18]. Unlike

the fluorene ring, the biphenyl group has a less planar and less rigid structure since one benzene ring is slightly twisted with respect to the other with a dihedral angle. Nevertheless, the insertion of the biphenyl unit can extend  $\pi$ -conjugation of fluorene system to promote liquid crystallinity [19]. The reactive mesogenic molecules containing fluorene and biphenyl groups as well as the thiophene oligomers based on fluorene were synthesised and their LC properties were investigated with high EL efficiency [20,21]. There seems to be little investigation of ‘polarised’ emission properties except for several literatures [6,8].

The technologies for the high polarised emission include not only energy transfer in host-guest system but also uniform alignment of emitting and/or hole injection layer (HIL) [20,22–25]. Particularly, thermal annealing process of mesogenic compounds in their LC phase may be necessary to induce the optimally uniform alignment. Adopting the small molecules instead the oligomers

**CONTACT** E-Joon Choi ✉ [ejchoi@kumoh.ac.kr](mailto:ejchoi@kumoh.ac.kr); Chang-Jae Yu ✉ [cjyu@hanyang.ac.kr](mailto:cjyu@hanyang.ac.kr)

\*These authors contributed equally to this work.

or polymers based on the fluorene seems to attractive approach since the former can achieve more easily spontaneous alignment than the latter. However, in case of a fairly low molecular weight compounds, 9,9-dialkyl substitution at the bridging methylene can give rise to the severely low axial ratios that may adversely affect the formation of the LC phase. Therefore, the trade-off approach is to design the smallest molecules with the fluorene and biphenyl groups which can form the mesophase, and to retain the emitting property with a high polarisation ratio (PR).

In this study, the luminescent compounds with a quite low molecular weight have been synthesised by a Suzuki coupling reaction (Scheme 1). The low aspect ratio mesogen with fluorene and biphenyl moieties was designed, which was connected to terminal pentyloxy group as well as lateral propyl or octyl group. Structure of compounds was identified by using  $^1\text{H-NMR}$  spectrometry and an elementary analysis, thermal and LC properties were evaluated by DSC method and POM observation, and absorption and luminescent properties were investigated by UV-vis, photoluminescence (PL) and EL spectrometry. Sequentially, the mesomorphic and the resultant anisotropic luminescent properties (i.e. the PR, were investigated in both PL and EL). We aligned the obtained LC compounds to the rubbing direction after spin-coating and examined alignment characteristics of the luminescent molecules. The uniformity of alignment was confirmed using a polarising microscopic texture, and the retardation was evaluated using a photoelastic modulator.

## 2. Experimental

### 2.1. Materials and general instrumentation

Pentyloxybiphenyl-4-boronic acid, 2,7-dibromo-dipropylfluorene and 2,7-dibromo-9,9-dioctylfluorene were used as received from TCI. Tetrakis(triphenylphosphine)-

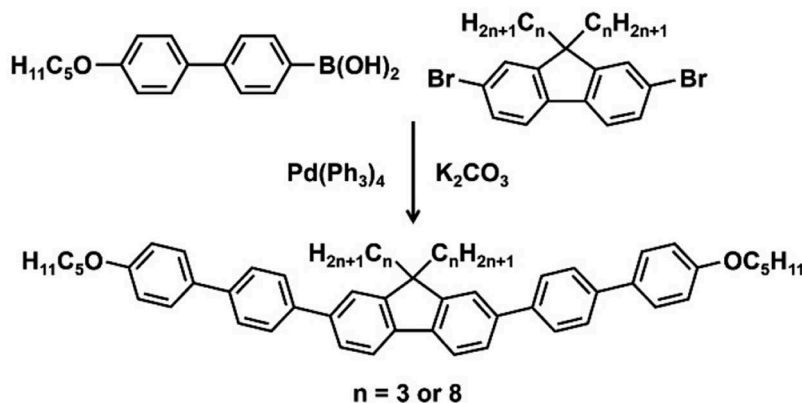
palladium(0) was used as received from G-ored Company. Potassium carbonate, magnesium sulphate, dichloromethane, tetrahydrofuran and acetone were used as received from Dae-Jung Chemical Co. Silica gel for column chromatography was used as received from Merck. NMR spectra were obtained by Bruker Biospin 400 MHz NMR spectrometers. Elemental analysis was performed with a Thermo Fisher Flash 2000. The thermal transition temperatures were determined by differential scanning calorimeter (NETZSCH DSC 200 F3). DSC measurements were performed in a  $\text{N}_2$  atmosphere with heating and cooling rates of  $10^\circ\text{C min}^{-1}$ . Optical textures obtained on no surface treatments were observed by a polarising microscope (Carl Zeiss Axioskop 40 Pol) equipped with a camera and a thermo controller (Mettler FP82HT). UV-vis absorption spectra were recorded on an Optizen 3220UV spectrometer.

### 2.2. Synthesis of small mesogenic molecules

The compounds were prepared according to procedures in the literature with a modification [21].

#### 2.2.1. Synthesis of compound 1

Tetrakis(triphenylphosphine)palladium(0) (0.16 g, 0.1 mmol) was added to a stirred solution of 4'-pentyloxybiphenyl-4-boronic acid (1.6 g, 5.6 mmol), 2,7-dibromo-9,9-dipropylfluorene (1.15 g, 2.8 mmol) and a 13% aqueous potassium carbonate solution (5 L) in THF (100 L) at room temperature. The reaction mixture was stirred for 24 h under reflux. The cooled reaction mixture was added to water (300 L) and the product was extracted into DCM ( $2 \times 200$  L), dried ( $\text{MgSO}_4$ ) and filtered. After evaporation, the residue was purified by column chromatography on silica gel using a mixture of DCM/hexane (3:2 v/v) as an eluent and recrystallisation from acetone to afford the solid product. Yield: 30%.  $^1\text{H NMR}$  ( $\text{CDCl}_3$ ,  $\delta_{\text{H}}$  in



**Scheme 1.** Synthesis of liquid crystalline light emitting compounds.

ppm): 0.68 (t,  $J = 8$  Hz, 6H), 0.73–0.79 (m, 4H), 0.93 (t,  $J = 8$  Hz, 6H), 1.38–1.46 (m, 8H), 1.79–1.82 (m, 4H), 2.01–2.05 (m, 4H), 4.00 (t,  $J = 8$  Hz, 4H), 7.57 (t,  $J = 6$  Hz, 4H), 7.64 (t,  $J = 6$  Hz, 8H), 6.98 (d,  $J = 8$  Hz, 4H), 7.72 (d,  $J = 8$  Hz, 4H), 7.76 (d,  $J = 8$  Hz, 2H). Elemental analysis calculated for  $C_{53}H_{58}O_2$ : C 87.56, H 8.04; Found: C 87.89, H 8.88%.

### 2.2.2. Synthesis of compound 2

Quantities: tetrakis(triphenylphosphine)palladium(0) (0.12 g, 0.1 mmol), 4'-pentyloxy-biphenyl-4-boronic acid (2 g, 7.0 mmol) and 2,7-dibromo-9,9-dioctylfluorene (1.93 g, 3.5 mmol). The experimental procedure was as described for the preparation of compound 1. The crude product was purified by column chromatography (silica gel; DCM/hexane 3:2 v/v) and recrystallisation from a mixture of acetone/water (9:1 v/v) to afford the desired product. Yield: 16%.  $^1H$  NMR ( $CDCl_3$ ,  $\delta_H$  in ppm): 0.77 (t,  $J = 8$  Hz, 10H), 0.93 (t,  $J = 8$  Hz, 6H), 1.05–1.17 (m, 20H), 1.36–1.48 (m, 8H), 1.77–1.84 (m, 4H), 2.01–2.05 (m, 4H), 4.00 (t,  $J = 8$  Hz, 4H), 6.98 (d,  $J = 8$  Hz, 4H), 7.57 (d,  $J = 9$  Hz, 4H), 7.59–7.63 (m, 4H), 7.64 (d,  $J = 8$  Hz, 4H), 7.72 (d,  $J = 8$  Hz, 4H), 7.77 (d,  $J = 8$  Hz, 2H). Elemental analysis calculated for  $C_{63}H_{78}O_2$ : C 87.25, H 9.07; Found: C 87.14, H 9.46%.

### 2.3. Device fabrication

The OLEDs with the small mesogenic compounds synthesised for an emitting layer (EML) were fabricated in this work. The device structures and energy diagram are shown in Figure 1. After rinsing prepatterned indium-tin-oxide (ITO) substrates in an ultrasonic bath with deionised water and mucasol (alkali detergent) for 60 min, the ITO substrates were treated with  $O_2$  plasma to improve the adhesion of poly(3,4-ethylenedioxythiophene): polystyrene sulfonate (PEDOT:PSS from LUMTEC). Here, the PEDOT:PSS acts as a HIL as well as an alignment layer for the mesogenic EML. The PEDOT:PSS was spin-coated (at 1000 rpm for 10 s

and 3000 rpm for 20 s) on the plasma-treated ITO substrate and unidirectionally rubbed by a rubbing machine [26] after baking at 100°C for 10 min. The dissolved small mesogenic compounds in toluene (17.7 mg/mL) was spin-coated (at 1000 rpm for 10 s and 3000 rpm for 20 s) on the rubbed PEDOT:PSS and dried at room temperature. The thickness of the EML with the small mesogenic compounds was measured to be 80 nm.

The EML film was prepared with thermal treatment of rapidly quenching process (with liquid nitrogen) after annealing at 140°C for 30 s. The reference EML film was prepared without any thermal treatment. Finally, 2,2',2''-(1,3,5-benzinetriyl)-tris(1-phenyl-1H-benzimidazole) (TPBi, 20 nm), LiF (1 nm), Al (70 nm) were sequentially deposited by high-vacuum ( $6 \times 10^{-6}$  torr) thermal evaporation as an electron-transporting layer, electron injection layer (EIL), and cathode, respectively. All process is carried out in glove box filled with nitrogen gas and the EL samples were additionally encapsulated by glass to avoid exposure to humidity and oxygen.

### 2.4. Device characterisation

The linearly polarised (LP) PL and EL of the OLEDs were measured by a spectroradiometer (SR-UL1R from TOPCON). The LPPL and LPEL spectra were measured under a linear polariser at 0° and 90° with respect to the rubbing direction of the PEDOT:PSS. The PL quantum efficiency for the spin-coated compound on the rubbed alignment layer was measured using the spectrofluorometer (FP-8500 from JASCO). The current density-voltage-luminance (J-V-L) characteristics of the OLEDs were evaluated using a source meter (Keithley 2000 from Keithley Instruments) and spectroradiometer. The retardation of the EML was measured with photoelastic modulator (PEM) (PEM-100 from Hinds) and lock-in amplifier (SR830 from Stanford Research System) based on the PEM method [27]. Microscopic textures were observed under a polarising optical microscope (POM) (E600W POL from Nikon) with frame-grabbing system (SDC-450 from Samsung). All measurements were carried out in ambient environments after encapsulation.

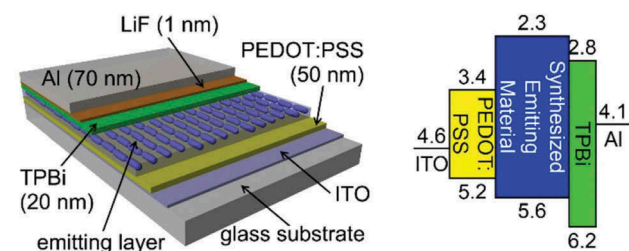


**Figure 1.** (Colour online) EL device structure and energy level diagram of the OLED.

## 3. Results and discussion

### 3.1. Thermal properties

Figure 2 shows the DSC thermograms of the compounds, and Table 1 presents their transition temperatures and enthalpy changes. Compounds 1 and 2

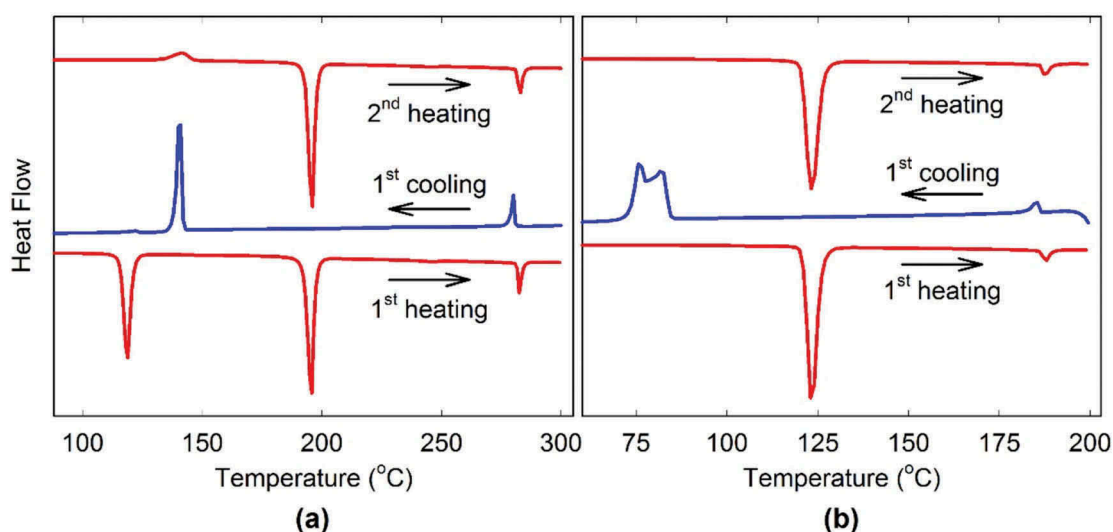


**Figure 2.** (Colour online) DSC curves for the first heating, the first cooling, and the second heating (scan rate of  $10^{\circ}\text{C min}^{-1}$ ) of (a) the compound **1** ( $n = 3$ ) and (b) the compound **2** ( $n = 8$ ).

**Table 1.** Transition temperatures ( $T$ ,  $^{\circ}\text{C}$ ) and enthalpy changes ( $\Delta H$ ,  $\text{kJ mol}^{-1}$ ) of compounds.<sup>a</sup>

Compound	DSC run	$T_{k-k}$	$\Delta H_{k-k}$	$T_c$	$\Delta H_c$	$T_m$	$\Delta H_m$	$T_i$	$\Delta H_i$
1 ( $n = 3$ )	1-heating	119	29.2			196	36.3	283	3.9
	1-cooling			141	23.3			280	4.1
	2-heating					196	36.2	283	3.9
2 ( $n = 8$ )	1-heating					123	39.5	188	1.6
	1-cooling			76, 82	33.5			185	1.7
	2-heating					123	38.1	188	1.5

<sup>a</sup>Abbreviations of subscript: k-k: solid-to-solid transition; c: crystallising transition; m: melting transition; i: isotropic transition.

showed the melting and isotropisation transitions on both heating and cooling. The melting ( $T_m$ ) and isotropisation temperature ( $T_i$ ) of compound **2** with a longer end group was lower than that of compound **1** with a shorter end group. The enthalpy changes for melting ( $\Delta H_m$ ) of the two compounds were not very different in the values and were about  $40 \text{ kJ mol}^{-1}$ . Unlike the  $\Delta H_m$ , the enthalpy changes for isotropisation ( $\Delta H_i$ ) are relatively largely different depending on the structure, and the  $\Delta H_i$  of compound **1** is more than twice times higher than that of compound **2**. The DSC results indicate that compound **2** with propyl lateral group can have lower melting temperature than compound **1** with octyl one. Instead, the latter can form the more thermodynamically stable mesophase than the former.

Moreover, depending on the DSC running cycles, only little change was observed in the all transition temperature and enthalpy changes for two compounds except for the distinctive solid-to-solid transitions in compound **1** on the first heating cycle. This implies that the major transition behaviours of compounds scarcely depend on the thermal hysteresis.

### 3.2. Optical properties

The UV absorption and the PL properties of two compounds have been observed. The absorption and the PL spectra of two compounds in  $\text{CHCl}_3$  solvent are shown in Figure 3. The wavelengths of the maximum absorption, the onset absorption, and the wavelengths of the maximum PL of each compound were summarised in Table 2. Although two compounds have different lengths of the flexible end group, both compounds exhibited the same absorption spectra with the

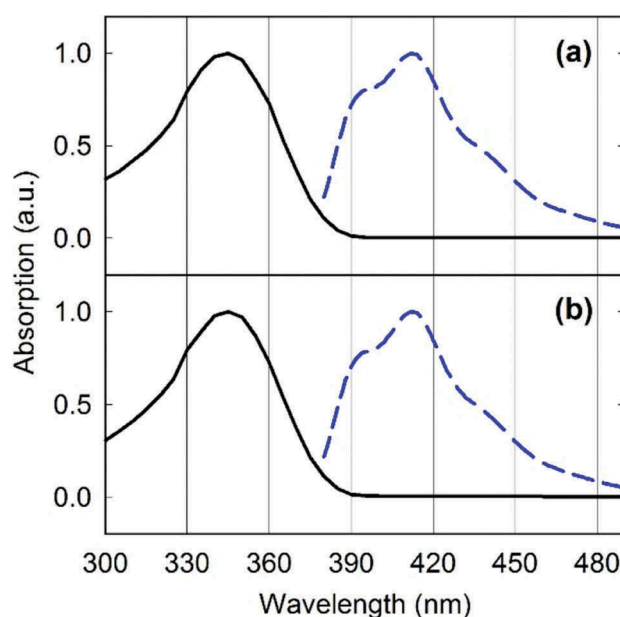


**Figure 3.** (Colour online) Absorption spectra (solid lines) and PL spectra (dashed lines) of (a) the compound **1** and (b) the compound **2** in  $\text{CHCl}_3$  solvent.

**Table 2.** Photophysical properties of compounds.

Compound	$\lambda_{\max}^{Abs}$ (nm)	$\lambda_{\text{onset}}^{Abs}$ (nm)	$E_g^{opt}$ (eV)	$\lambda_{\max}^{PL}$ (nm)	$^a\eta_{\text{ext}}^{PL}$ (%)
1 (n = 3)	345	380	3.26	412	14.2
2 (n = 8)	345	380	3.26	412	15.1

<sup>a</sup>The external quantum efficiency was measured with the spin-coated compounds on rubbed alignment layer.

maximum absorption at 345 nm and the onset absorption at 380 nm since they have the same rigid core groups. The optical band gap ( $E_g^{opt}$ ) was determined by measuring the onset value of the absorption spectrum, and was calculated to be 3.26 eV using the Planck relation. The PL external quantum efficiency of compound **2** was a little greater than that of compound **1** without thermal treatment.

Figure 4 shows the optical textures of two compounds on the untreated substrate observed by the POM under crossed polarisers. Both compounds exhibited nematic brushes or threaded (i.e. schlieren) textures. The DSC and POM results indicate that both compounds formed an enantiotropic nematic mesophase on heating and cooling processes.

### 3.3. Properties of LP emission

The luminescent mesogenic compounds spontaneously emitted PL or EL light with a high PR due to their self-

orientational ordering on an anisotropically treated substrate. The OLED devices for investigating the LP emission of the synthesised compounds were fabricated as shown in Figure 1. To promote uniformity of alignment for mesogenic compounds **1** and **2** acting as the EML, the PEDOT:PSS acting as the HIL was rubbed, and two solutions of mesogenic compounds dissolved in toluene were spin-coated on the rubbed PEDOT:PSS, individually.

#### 3.3.1. Anisotropy on rubbed substrate

Figure 5 shows the POM images and the birefringence of the spin-coated mesogenic compounds **1** and **2** on the rubbed PEDOT:PSS substrate at room temperature. It should be noted that although the compounds were dissolved in toluene and spin-coated at room temperature on the rubbed substrate, both compounds exhibited an anisotropic textures even below the mesogenic temperature. In the compound **1**, random light-leaking spots are observed when the rubbing direction is parallel to one of crossed polarisers, and the random dark patterns are observed when the rubbing direction is rotated by 45° from the polariser as shown in Figure 5(a). On the other hand, good dark texture is obtained in the compound **2** when the rubbing direction is parallel to one of crossed polarisers as shown in Figure 5(b). Such textures imply that the compound **2** is better aligned

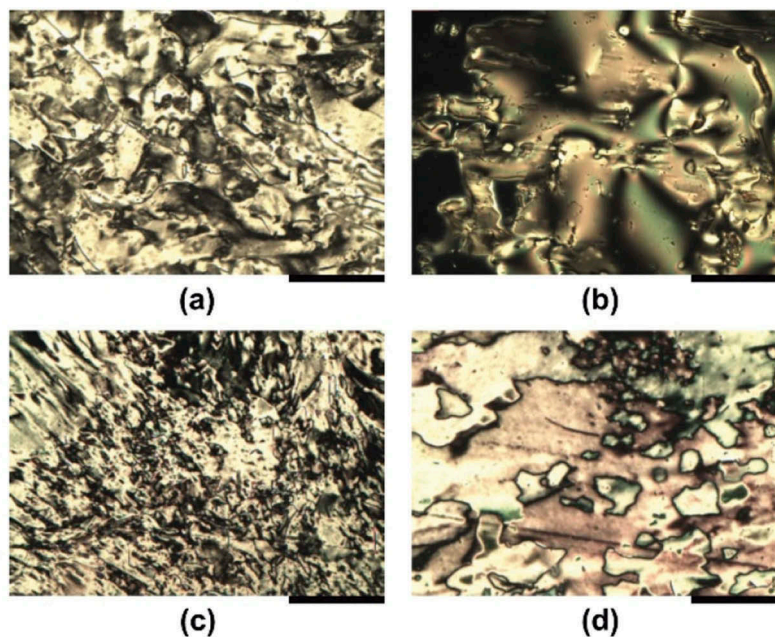


**Figure 4.** (Colour online) Microscopic textures under crossed polarisers at (a) 238°C on heating process and (b) 273°C on cooling process of the compound **1**, and at (c) 186°C on heating process and (d) 135°C on cooling process of the compound **2** on the untreated substrates. A scale bar represents 25  $\mu\text{m}$ .

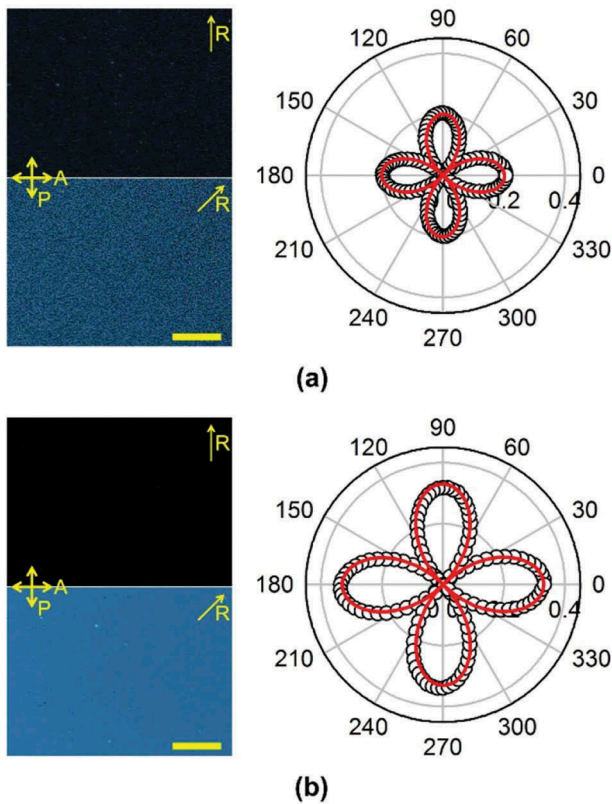


**Figure 5.** (Colour online) Microscopic textures under crossed polarisers and measured phase retardations using PEM method of (a) the compound **1** and (b) the compound **2** spin-casted on the rubbed PEDOT:PSS layer. Here, the letters 'P', 'A', and 'R' represent the polariser, analyser, and rubbing directions, respectively. All textures were taken in the same scale (a scale bar represents 100  $\mu\text{m}$ ). The least-square-fits of the retardation are depicted by solid lines.

than the compound **1**, and thus the former has greater birefringence than the latter under similar.

The birefringence of the aligned mesogenic compounds was determined by measuring the phase retardation  $B$  as a function of the rotation angle  $\theta$  with respect to one of the crossed polariser in the PEM method [27]. The measured phase retardations (symbols) were fitted by the following equation [26,28],

$$B(\theta) = \left[ \frac{2 \sin \theta B_0 \cos 2\theta}{1 - \cos 4\theta + \cos B_0 (1 + \cos 4\theta)} \right] \quad (1)$$

Here, the fitting parameter  $B_0 (=2\pi d\Delta n/\lambda)$  is an effective phase retardation of the mesogenic compounds with thickness  $d$  ( $=80$  nm) and birefringence  $\Delta n$  at wavelength  $\lambda$  ( $=410$  nm). As shown in Figure 5, the effective phase retardation of the compounds **1** and **2** were obtained to be 0.20, and 0.33, respectively. Finally, the birefringence of the compound **1** was calculated to be 0.16 and that of the compound **2** was 0.27. It should be noted that the optical properties of both compounds

are similar to each other as shown in Figure 3 and Table 2. Higher birefringence implies higher ordering of the mesogenic compound and higher degree of the LP emission [26,29]. As a result, the compound **2** is better aligned than the compound **1** on the rubbed PEDOT:PSS as shown in microscopic textures under crossed polarisers in Figure 5.

### 3.3.2. LP emission

Figure 6 shows the PL and EL spectra of the compound **1** and **2** on the rubbed PEDOT:PSS layer. Each spectrum was measured under linear polariser parallel (solid lines) and perpendicular (dashed lines) to the rubbing direction. Even in both reference samples prepared with the compound **1** (a, b) and **2** (c, d) without thermal annealing process at their mesogenic phases for unidirectional alignment, the polarised emissions were observed as shown in Figure 6(a–d). In the dissolved compounds in toluene, molecular interaction between mesogenic compounds is diminished and the anisotropic alignment was generated on the rubbed alignment layer. In Table 3, the LP ratio is defined by the ratio of luminous intensities polarised parallel and perpendicular to the rubbed direction. The LPPL and LPEL ratios of the compound **1** at peak intensity were measured to be 2.83 and 3.95, respectively. Similarly, the LPPL and LPEL ratios of the compound **2** were 4.27 and 5.68, respectively. However, the compound **1** exhibited rapid degradation of both PL and EL emissions. In addition, the compound **1** devices were seriously damaged by the thermal annealing process due to its higher mesogenic temperature.

We prepared the thermal annealed samples with the compound **2** to investigate an enhancement of the LP ratio. As mentioned above, the reference samples were fabricated at room temperature, where the compound **2** did not exhibit the mesogenic phase according to  $T_m$  defined by DSC. To improve the self-alignment property of the compound **2**, the PL and EL samples were heated up to 140°C after spin-coating the compound **2**, and rapidly quenched with liquid nitrogen after annealing at 140°C for 30 s. Then, the LPPL (e) and LPEL (f) ratios of the thermally annealed compound **2** at peak intensity were measured to be 11.56 and 14.89, respectively. This result indicates that the LP ratios of both PL and EL lights can be increased more twice than ones of the reference samples conventionally by using the thermal annealing process.

The luminance efficiency of the OLED samples with/without thermal annealing process was characterised with the J-V-L measurements. Figure 7 shows the current density and luminance as a function of an applied voltage, and efficiency of the spin-casted compounds on the rubbed PEDOT:PSS layer. In Table 3,

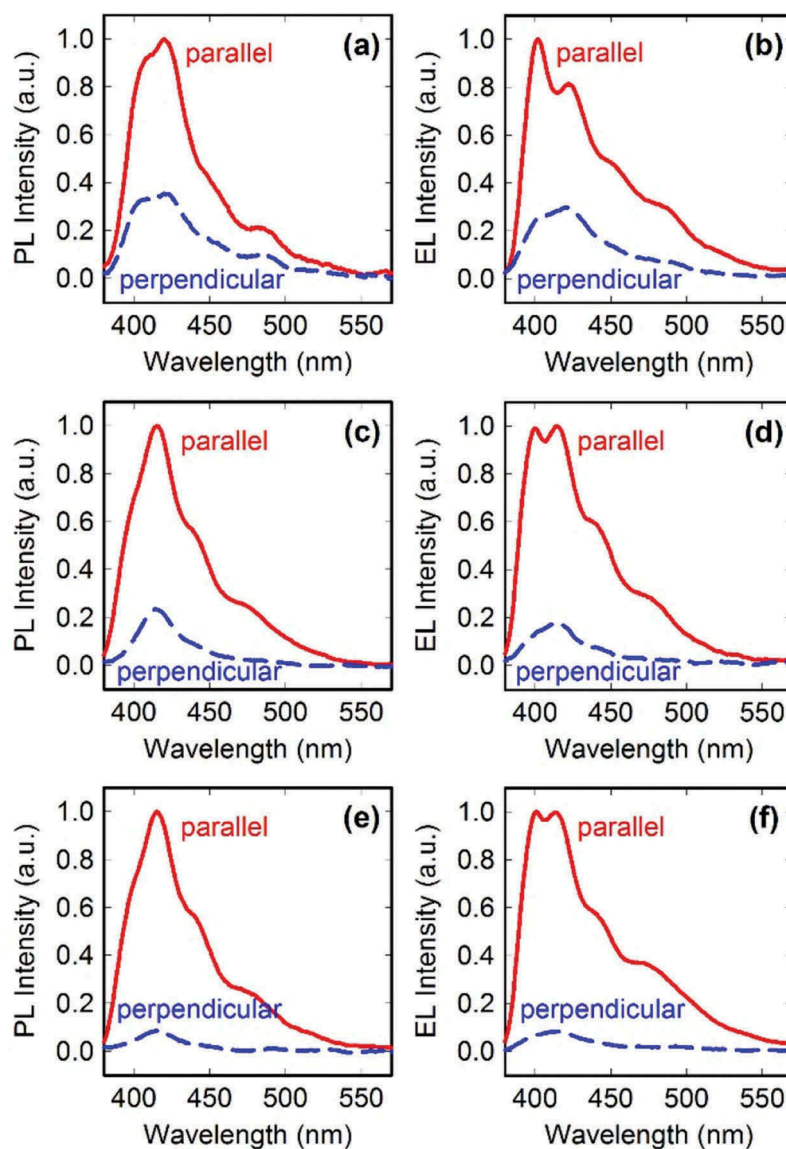


**Figure 6.** (Colour online) PL and EL spectra of the compound **1** (a, b) and the compound **2** (c, d) spin-casted on the rubbed PEDOT:PSS layer without thermal annealing process, and the compound **2** (e, f) quenched after thermal annealing at its LC phase. Each spectra were measured under linear polariser parallel and perpendicular to the rubbing direction of the PEDOT:PSS layer.

**Table 3.** EL and linear-polarisation properties for compounds.

Compound	Thermal treatment	Turn-on voltage <sup>a</sup> (V)	Maximum efficiency (cd A <sup>-1</sup> )	LPPL <sup>b</sup>	LPEL <sup>c</sup>
1	As-prepared	6.5	0.88	2.83	3.95
2	As-prepared	5.5	1.53	4.27	5.68
2	Annealed <sup>d</sup>	6.5	0.33	11.56	14.89

<sup>a</sup>Voltage was measured at 1 cd/m<sup>2</sup>.

<sup>b</sup>Polarisation ratio for PL.

<sup>c</sup>Polarisation ratio for EL.

<sup>d</sup>EML films were rapidly quenched after annealing at 140°C for 30 s.

for as-prepared compound **1**, the maximum efficiency was measured to be 0.88 cd/A. Without thermal annealing process, compound **2** showed smaller turn-on voltage but higher efficiency than compound **1**, respectively. As mentioned above, compound **2** exhibited more reliable against thermal treatment than compound **1**. Moreover, we have measured luminance

efficiency of compound **2** quenched after thermal annealing process under the LC phase. After thermal treatment, the maximum current density was almost similar, but the luminance decreased to less than half as shown in Figure 7(c). By using thermal annealing process, although the luminance efficiency was reduced due to the void sites where no light was emitted when

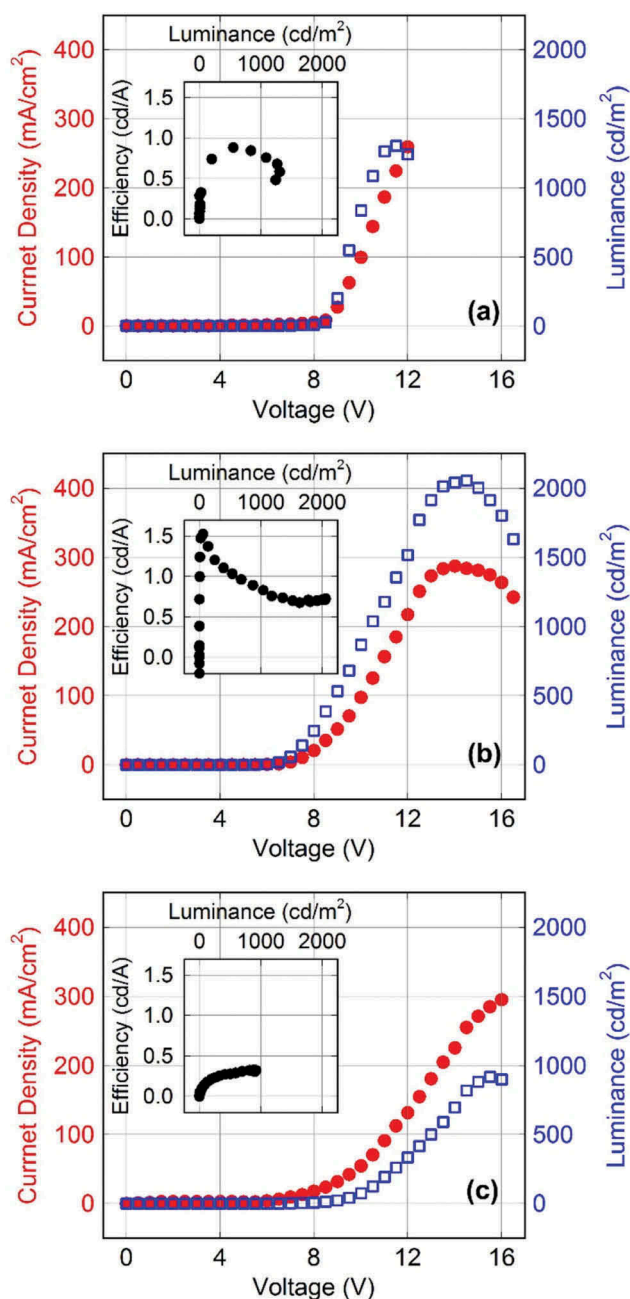


**Figure 7.** (Colour online) Current density (filled circles) and luminance (open squares) versus voltage characteristics, and efficiency (insets) of (a) the compound **1** and (b) the compound **2** spin-casted on the rubbed PEDOT:PSS layer without thermal annealing process, and (c) the compound **2** quenched after thermal annealing at its LC phase.

the current flowed, the LP ratios of both PL and EL lights can be increased more twice than ones of the reference samples. As a result, the first objective of this study, which is a demonstration of the relatively high LP ratios based on low aspect ratio mesogenic molecules, was achieved because the emitting material exhibited mesogenic phase and thus its alignment property was improved.

## 4. Conclusions

We have synthesised new luminescent rod-like molecules using a Suzuki coupling reaction, which contain a low aspect ratio mesogenic core with the fluorene and biphenyl moieties. First of all, we found that compounds formed an enantiotropically thermotropic nematic mesophase.

Regarding mesogenic luminescent materials, in general, one way to increase the optical anisotropy is to increase the aspect ratio of the molecules. In this case, the one important issue is ‘How high aspect ratio can be optimal for manifesting anisotropic properties?’ One of the methods to increase the aspect ratio of rod-like molecules is to increase the molecular weight of the molecule. That is, when the mesogenic molecules are made into oligomers or polymers, the aspect ratio increases and manifestation of anisotropy is guaranteed. So far, most studies have been made mainly in the direction of increasing the aspect ratio, that is, in the direction of increasing the molecular weight.

On the other hand, generally, in the case of the fluorene system, in order to increase the solubility, the lateral alkyl substituents should be introduced at the position of 9,9-position, so that the aspect ratio is reduced to fatal against LC formation. In this case, the important issue is ‘How low aspect ratio can retain the effective anisotropic properties?’ Therefore, in this study, the unique structure with the lowest aspect ratio structural unit was chosen by us. The minimum length of mesogenic structural unit can be accomplished by insertion of two biphenyl groups into 2,7-position of a central fluorene core, which were connected into the pentyloxy end group. In addition, propyl and octyl lateral substituents were introduced to 9,9-position of the central fluorene core in order to finely adjust the aspect ratio. As expected, the transition temperatures of compound **2** with octyl group were lowered than that of compound **1** with propyl group. However, according to the enthalpy changes, the thermodynamic stability of the nematic mesophase for the former was higher than that of the latter. Nonetheless, it should be noted that the ‘glassy’ nematic phase could be formed during the spin-coating with the toluene solution of compounds onto the rubbed HTL layer. Here, compound **2** with octyl group had better orientation properties than the compound **1** with propyl group. Further, the degree of orientation was improved at the time of heat treatment, so that the effective increasing the PL could be achieved only in compound **2**.

We believed that the pentyloxy end group may lead to reduce rotational viscosity and the octyl lateral group, instead propyl, may induce the proper aspect ratio of mesogen so that the melting temperature can be controlled minutely without losing the anisotropic character.

As a result, the optimally reduced aspect ratio of compound **2** led LPPL and LPEL somewhat high by 4.27 and 5.68, respectively, even in spin-coated on a rubbed HIL layer without a thermal annealing process. Moreover, interestingly enough, the LPPL and LPEL was significantly enhanced to be 11.56 and 14.89, respectively, by the thermal annealing process on the rubbed HIL layer.

## Disclosure statement

No potential conflict of interest was reported by the authors.

## Funding

This work supported by KDRC (Korea Display Research Consortium) support program for the development of future devices technologies for display industry.

## References

- [1] Hu G, Billa MR, Kitney SP, et al. Symmetrical carbazole-fluorene-carbazole nematic liquid crystals as electroluminescent organic semiconductors. *Liq Cryst.* **2018**;45(7):965–979.
- [2] Zou G, Luo KJ, Zhao L, et al. Ortho-platinated metallo-mesogens based on rod mesogenic unit of 2-phenylpyridine derivatives: synthesis, high linearly polarised and phase-state-dependent luminescence. *Liq Cryst.* **2018**;45(4):593–606.
- [3] Aguiar LD, Regis E, Tuzimoto P, et al. Investigation of thermal and luminescent properties in 4,7-diphenylethynyl-2,1,3-benzothiadiazole systems. *Liq Cryst.* **2018**;45(1):49–58.
- [4] Singh G, Fisch MR, Kumar S. Tunable polarised fluorescence of quantum dot doped nematic liquid crystals. *Liq Cryst.* **2017**;44(3):444–452.
- [5] Olate FA, Parra ML, Vergara JM, et al. Star-shaped molecules as functional materials based on 1,3,5-benzenetriesters with pendant 1,3,4-thiadiazole groups: liquid crystals, optical, solvatochromic and electrochemical properties. *Liq Cryst.* **2017**;44(7):1173–1184.
- [6] Culligan SW, Geng Y, Chen SH, et al. Strongly polarized and efficient blue organic light-emitting diodes using monodisperse glassy nematic oligo(fluorene)s. *Adv Mater.* **2003**;15:1176–1180.
- [7] Chen ACA, Culligan SW, Geng Y, et al. Organic polarized light-emitting diodes via Förster energy transfer using monodisperse conjugated oligomers. *Adv Mater.* **2004**;16:783–788.
- [8] Del Barrio J, Chinelatto LS, Serrano JL, et al. Extended liquid-crystalline oligofluorenes with photo- and electroluminescence. *New J Chem.* **2010**;34:2785–2795.
- [9] Liu S-H, Lin M-S, Chen L-Y, et al. Polarized phosphorescent organic light-emitting devices adopting mesogenic host-guest systems. *Org Electron.* **2011**;12:15–21.
- [10] Sanchez I, Mayoral MJ, Ovejero P, et al. Luminescent liquid crystal materials based on unsymmetrical boron difluoride  $\beta$ -diketonate adducts. *New J Chem.* **2010**;34:2937–2942.
- [11] O'Neill M, Kelly SM. Ordered materials for organic electronics and photonics. *Adv Mater.* **2011**;23:566–584.
- [12] Lee D-M, Song J-W, Lee Y-J, et al. Control of circularly polarized electroluminescence in induced twist structure of conjugate polymer. *Adv Mater.* **2017**;29:1700907.
- [13] Wang Y, Shi J, Chen J, et al. Recent progress in luminescent liquid crystal materials: design, properties and application for linearly polarised emission. *J Mater Chem C.* **2015**;3:7993–8005.
- [14] Honma M, Horiuchi T, Nose T, et al. Oblique extraction of polarized light from light-emitting liquid crystal cells doped with a fluorescent dye. *Jpn J Appl Phys.* **2013**;52(7R):070205.
- [15] Marcelo NF, Vieira AA, Cristiano R, et al. Polarized light emission from aligned luminescent liquid crystal films based on 4,7-disubstituted-2,1,3-benzothiadiazoles. *Synth Met.* **2009**;159:675–680.
- [16] Leclerc M. Polyfluorenes: twenty years of progress. *J Polym Sci Part A Polym Chem.* **2001**;39:2867–2873.
- [17] Scherf U, List EJW. Semiconducting polyfluorenes-towards reliable structure-property relationships. *Adv Mater.* **2002**;14:477–487.
- [18] Grimsdale AC, Chan KL, Martin RE, et al. Synthesis of light-emitting conjugated polymers for applications in electroluminescent devices. *Chem Rev.* **2009**;109:897–1091.
- [19] Davison IR, Hall DM, Sage I. Fluorene analogues of biphenyls: comparison of mesogenic behaviour. *Mol Cryst Liq Cryst.* **1985**;129:17–35.
- [20] Aldred MP, Eastwood AJ, Kelly SM, et al. Light-emitting fluorene photoreactive liquid crystals for organic electroluminescence. *Chem Mater.* **2004**;16:4928–4936.
- [21] Kitney SP. Liquid crystalline semiconductors for organic electronics. Hull, UK: University of Hull; **2008**.
- [22] Contoret AEA, Farrar SR, O'Neill M, et al. The photopolymerization and cross-linking of electroluminescent liquid crystals containing methacrylate and diene photopolymerizable end groups for multilayer organic light-emitting diodes. *Chem Mater.* **2002**;14:1477–1487.
- [23] Woon KL, O'Neill M, Richards GJ, et al. Highly circularly polarized photoluminescence over a broad spectral range from a calamitic, hole-transporting, chiral nematic glass and from an indirectly excited dye. *Adv Mater.* **2003**;15:1555–1558.
- [24] Aldred MP, Contoret AEA, Farrar SR, et al. A full-color electroluminescent device and patterned photoalignment using light-emitting liquid crystals. *Adv Mater.* **2005**;17:1368–1372.
- [25] Aldred MP, Vlachos P, Contoret AEA, et al. Linearly polarised organic light-emitting diodes (OLEDs): synthesis and characterisation of a novel hole-transporting photoalignment copolymer. *J Mater Chem.* **2005**;15:3208–3213.
- [26] Jung J-H, Lee D-M, Kim J-H, et al. Circularly polarized electroluminescence by controlling the emission zone in a twisted mesogenic conjugate polymer. *J Mater Chem C.* **2018**;6:726–730.
- [27] Hinds Instruments. PEM-100 Technical Note.
- [28] Lee J-H, Yu C-J, Lee S-D. A novel technique for optical imaging of liquid crystal alignment layers. *Mol Cryst Liq Cryst.* **1998**;321:317–322.
- [29] Lee D-M, Y-J KL, Kim J-H, et al. Birefringence-dependent linearly-polarized emission in a liquid crystalline organic light emitting polymer. *Opt Exp.* **2017**;25:3737–3742.